THE JOURNAL OF BIOLOGICAL CHEMISTRY VOL. 285, NO. 22, pp. 17177–17187, May 28, 2010
© 2010 by The American Society for Biochemistry and Molecular Biology, Inc. Printed in the U.S.A.

α-AP-2 Directs Myosin VI-dependent Endocytosis of Cystic Fibrosis Transmembrane Conductance Regulator Chloride Channels in the Intestine*[S]

Received for publication, March 26, 2010 Published, JBC Papers in Press, March 29, 2010, DOI 10.1074/jbc.M110.127613

Anne Collaco[‡§], Robert Jakab[‡§], Peter Hegan[¶], Mark Mooseker[¶], and Nadia Ameen[‡§1]

From the [‡]Departments of Pediatrics and Cell Biology University of Pittsburgh School of Medicine, Pittsburgh, Pennsylvania 15206 and the Departments of [§]Pediatrics and [¶]Molecular, Cellular, and Developmental Biology, Yale University, New Haven, Connecticut 06520

The actin motor myosin VI regulates endocytosis of cystic fibrosis transmembrane conductance regulator (CFTR) in the intestine, but the endocytic adaptor linking CFTR to myosin VI is unknown. Dab2 (Disabled 2) is the binding partner for myosin VI, clathrin, and α-AP-2 and directs endocytosis of low density lipoprotein receptor family members by recognizing a phosphotyrosine-binding domain. However, CFTR does not possess a phosphotyrosine-binding domain. We examined whether α-AP-2 and/or Dab2 were binding partners for CFTR and the role of myosin VI in localizing endocytic adaptors in the intestine. CFTR co-localized with α-AP-2, Dab2, and myosin VI and was identified in a complex with all three endocytic proteins in the intestine. Apical CFTR was increased in the intestines of Dab-2 KO mice, suggesting its involvement in regulating surface CFTR. Glutathione *S*-transferase pulldown assays revealed binding of CFTR to α-AP-2 (but not Dab2) in the intestine, whereas Dab-2 interacted with α-AP-2. siRNA silencing of α-AP-2 in cells significantly reduced CFTR endocytosis, further supporting α-AP-2 as the direct binding partner for CFTR. α-AP-2 and Dab2 localized to the terminal web regions of enterocytes, but Dab2 accumulated in this location in Snell's Waltzer myosin VI$^{(sv/sv)}$ intestine. Ultrastructural examination revealed that the accumulation of Dab2 correlated with prominent involution and the loss of normal positioning of the intermicrovillar membranes that resulted in expansion of the terminal web region in myosin VI$^{(sv/sv)}$ enterocytes. The findings support α-AP-2 in directing myosin VI-dependent endocytosis of CFTR and a requirement for myosin VI in membrane invagination and coated pit formation in enterocytes.

The intestinal epithelium consists of a polarized monolayer of enterocytes that interface with the lumen on their apical membrane. Here, membrane transporters, nutrient receptors, and ion channels exert their various functions to maintain intestinal homeostasis (1). Cystic fibrosis transmembrane conductance regulator (CFTR)[2] chloride channels are present in enterocytes and are the major apical exit pathway for chloride and bicarbonate secretion into the lumen and thus critical to the pathogenesis of cystic fibrosis and secretory diarrhea (2, 3). The lack of CFTR on the apical membranes of enterocytes leads to dehydration and obstruction of the lumen by thick secretions that is associated with malabsorption in cystic fibrosis (4, 5). Conversely, accumulation of CFTR on the intestinal surface leads to increased fluid secretion and secretory diarrhea (6, 7).

Endocytosis of CFTR and its recycling back to the plasma membrane regulates the number of channels on the cell surface (8, 9). Under physiologic conditions, endocytic recycling also regulates CFTR anion transport on the apical membrane of epithelial cells (10). But emerging evidence indicates that endocytic recycling pathways traversed by CFTR in native epithelia are directed by tissue- and cell-specific binding partners (10–12). In the intestine, endocytic recycling regulates surface expression and CFTR-mediated anion transport (9, 10). But there is no information regarding binding partners that regulate endocytic trafficking of CFTR in the intestine.

Enterocytes in the small intestine are highly polarized, possessing a well developed brush border and abundant endocytic protein machinery that is necessary for receptor-mediated endocytosis. Here receptor-mediated endocytosis begins when a clathrin-coated pit forms on the intermicrovillar membrane in the region of the terminal web. Surface receptors are selected for endocytosis by adaptor proteins and migrate to the base of the microvilli where they are recruited to coated pits. Adaptors bind to clathrin and to internalization signals within cytoplasmic regions of the receptor. Once the clathrin coat is assembled, the membrane undergoes invagination and scission to form a clathrin-coated vesicle that moves away from the membrane to be internalized (13, 14).

In the small intestine, CFTR is on the microvillar membranes, in coated pits and clathrin-coated vesicles within the subapical cytoplasm of enterocytes (15). Myosin VI, a minus end-directed actin motor, is enriched in clathrin-coated structures in the terminal web region of enterocytes of the small intestine. This myosin regulates CFTR endocytosis, surface expression, and fluid secretion *in vivo* (6). However, myosin VI

* This work was supported, in whole or in part, by National Institutes of Health Grants R01 DK 077065 (to N. A.) and DK 25387 and GM 073823 (to M. M.).

[S] The on-line version of this article (available at http://www.jbc.org) contains supplemental Fig. S1.

[1] To whom correspondence should be addressed: Dept. of Pediatrics, Yale University School of Medicine, 333 Cedar St., FMP 408, New Haven, CT 06520. Tel.: 203-785-4649; Fax: 203-785-1384; E-mail: nadia.ameen@yale.edu.

[2] The abbreviations used are: CFTR, cystic fibrosis transmembrane conductance regulator; LDL, low density lipoprotein; PTB, phosphotyrosine-binding; GST, glutathione *S*-transferase; siRNA, small interfering RNA; PBS, phosphate-buffered saline; KO, knock-out; Myo 6, myosin VI.

lacks membrane-binding capability to enable engagement with CFTR or surface receptors directly, and the binding partner responsible for linking myosin VI to CFTR on the plasma membrane is unknown (13, 16). Furthermore, the specific site where myosin VI exerts its function in facilitating clathrin-mediated endocytosis is unknown (13). Myosin VI is also necessary for clathrin-mediated endocytosis of LDL surface receptors. In cells expressing members of the LDL surface receptor family, myosin VI promotes endocytosis through its endocytic binding partner Dab2 (Disabled 2). Dab2 directs endocytosis of LDL surface receptors by recognizing and binding to an F*X*NP*X*Y endocytic sorting motif via an N-terminal phosphotyrosine-binding (PTB) domain (17), whereas it binds to myosin VI more distally at its C terminus and to the endocytic machinery by engaging clathrin and the α appendage of the adaptor AP-2 within its central region (16–18).

Unlike members of the LDL receptor family, CFTR does not possess a PTB domain within its sequence to facilitate its engagement to Dab2. However, endocytosis of CFTR from the apical membrane in the small intestine is dependent on myosin VI(6). AP-2 was the first endocytic adaptor to be recognized. AP-2 consists of four subunits α, β_2, μ2, and σ2, that comprise the core of the complex. The α and β_2 subunits possess appendages or ears that are linked to the core by a hinge region. The AP-2 complex clusters cell surface receptors for endocytosis by forming a coat together with clathrin on the inside of the plasma membrane (19–21). Because Dab2 is a direct binding partner for myosin VI and α-AP-2 and apical endocytosis of CFTR in the intestine is dependent on myosin VI, we sought to determine whether Dab2 or α-AP-2 were physiologic binding partners for CFTR endocytosis in the intestine. We also examined whether myosin VI plays a role in localizing α-AP-2/Dab2 at the site of apical endocytosis in the intestine. It has been suggested that myosin VI may promote the endocytosis of receptors in polarized cells such as the small intestine by moving and positioning Dab2 at the site of coated pit formation on the plasma membrane, but direct evidence supporting such a role has not been provided.

MATERIALS AND METHODS

Reagents and Antibodies—The following antibodies were used in this study: CFTR (M3A7) (Chemicon International), CFTR 217 (Cystic Fibrosis Foundation Therapeutics), alkaline phosphatase (BYA1191) (Accurate Chemicals), AME 4991 CFTR(6), AP-2 α subunit monoclonal antibody (100/2) (Dr. Linton Traub, University Pittsburgh School of Medicine), α-Adaptin 1/2 (Santa Cruz Biotechnology, Inc.) Dab2 (H-110) (Santa Cruz Biotechnology, Inc.), clathrin monoclonal antibody (X-22) (Calbiochem, EMD Division Inc.), myosin 6 (KA-15), Dab2, p96 (BD Transduction Laboratories), rhodamine phalloidin (Invitrogen), fluorescein isothiocyanate-conjugated anti-rabbit and anti-mouse secondary (Invitrogen), Cy-3-conjugated anti-mouse secondary (Jackson Immuno Research Laboratories), and horseradish peroxidase-conjugated secondary antibodies (BD Bioscience). EZ-link sulfo-NHS-SS-biotin and immunopure immobilized streptavidin-agarose beads were obtained from Pierce. Lipofectamine™ 2000 reagent was purchased from Invitrogen. α-AP-2 siRNA was obtained from Dharmacon, Inc./Thermo Fisher Scientific. All other reagents were obtained from Sigma unless otherwise stated.

Animals—All of the studies were performed with the approval of the Institutional Animal Care and Use Committee of the University of Pittsburgh and the Yale University School of Medicine. Adult male Myo $6^{(sv/sv)}$ mice 6–8 weeks of age and heterozygote control Myo $6^{(sv/wt)}$ were obtained from Jackson Laboratories and Dr. Mark Mooseker (Yale University School of Medicine). When necessary, fasted mice were anesthetized using Avertin (2-2-2 Tribromoethanol; Sigma-Aldrich) 180 mg/kg administered by intraperitoneal injection. The mice were euthanized at the end of experiments using an overdose of Avertin. Overnight fasted adult male Sprague-Dawley rats (250–300 grams) were anesthetized with Inactin (120 mg/kg) by intraperitoneal injection and were euthanized at the end of the experiments using an overdose of Inactin. Intestinal tissues from Dab2 control (dab2 fl/−, cre/−) and knock-out (dab2 −/−, cre/+) mice were a generous gift from Dr. Jonathan Cooper (22).

Tissue Histology—Following fixation in paraformaldehyde (2% w/v) in PBS, jejunum from Dab2 control and knock-out (KO) mice were embedded in paraffin, and 4-μm-thick sections were mounted onto Superfrost-coated slides (Fisher). The sections were deparaffinized in xylene, dehydrated in 100 and 95% ethanol each for 5 min, rinsed in distilled water, and stained with hematoxylin for 1.5 min. Following hematoxylin staining, the sections were rinsed briefly with water, dehydrated in 70% ethanol, and then counterstained with eosin Y. The sections were dehydrated in 95 and 100% ethanol and incubated briefly in xylene; Permount was applied and sealed with a coverslip.

Transmission Electron Microscopy—Segments of proximal duodenum from age-matched (12 months) Myo $6^{(sv/wt)}$ and Myo $6^{(sv/sv)}$ mice were taken from saline-flushed intestine and fixed for 1 h in 2% glutaraldehyde (Electron Microscopy Science) 0.2% tannic acid, 0.1 M sodium phosphate, pH 7.0. The tissue was rinsed three times with 0.1 M sodium phosphate buffer, pH 7.0, and then post-fixed in 1% OsO4, 0.1 M sodium phosphate, pH 6.0. The tissue was then rinsed three times in cold H_2O and incubated on ice overnight in 1% uranyl acetate. The samples were then dehydrated in a graded series of ethanol, rinsed twice with propylene oxide, and incubated for 2 h each in 1:1, 3:1 and 1:0 (undiluted) mixtures of resin (EMbed 812; Electron Microscopy Science) and propylene oxide. The samples were then placed in fresh resin and baked for 1–2 days at 60 °C.

Cells—CaCo-2_{BB}e cells were obtained from ATCC and grown at 37 °C in 5% CO_2, 90% air atmosphere in high glucose with L-glutamine Dulbecco's modified Eagle's medium (Invitrogen), supplemented with 10% fetal bovine serum (Invitrogen), 10 μg/ml apo-transferrin (Chemicon International Temecula, CA), 1 mM/liter sodium pyruvate (Sigma), 1% penicillin-streptomycin (Invitrogen), 1 μg/ml Fungizone (Invitrogen), and 5 μg/ml Plasmocin (Invitrogen). The cells were seeded at 1×10^5 cells/cm^2 on 100-mm cell culture dishes (Corning Incorporated, Corning, NY), and passaged at 70% confluency on a 75-mm Transwell filters (Costar Inc.). Confluent monolayers of filter grown cells were used for immunoprecipitation and pulldown assays following 10–12 days of culture and transepithelial resistance greater than 300 ohm/

cm^2. Immunofluorescence labeling was performed on fully polarized cells seeded on 6.5-mm 0.4-μm pore size Transwell membranes (Corning). HEK 293 CFTR-expressing cells were a gift from Dr. Neil Bradbury (Chicago Medical School). The cells were grown in high glucose L-glutamine Dulbecco's modified Eagle's medium containing 10% fetal bovine serum (Invitrogen) and hygromycin B (150 μg/ml; Invitrogen) at 37 °C in 5% CO_2, 90% air atmosphere.

Immunofluorescence Microscopy of Tissues—Intestinal tissues were fixed in 2% (w/v) paraformaldehyde-PBS for 1 h at room temperature. The tissues were cryoprotected in 30% sucrose overnight in the cold and then embedded in Tissue-Tek O.C. T medium (Miles Laboratory) and frozen in liquid nitrogen-cooled isopentane. Cryostat sections (5 μm) were immunolabeled as described with minor modifications (6). Where necessary, antigen retrieval was performed by incubating sections with a heated solution of 0.05% citraconic anhydride, pH 7.4, for 1 h. Briefly, the sections were rehydrated in PBS, and nonspecific proteins were blocked with normal goat serum for 45 min and incubated with primary antibodies overnight at 4 °C. The sections were incubated with appropriate secondary antibodies for 1 h at room temperature, stained with 1% Hoechst nuclear solution and/or Draq 5 (1:1000 diluted in PBS), and mounted in Slow Fade medium (Molecular Probes). Where two polyclonal antibodies were employed on the same section, sequential labeling was performed as follows: the sections were immunolabeled with the first antibody overnight at 4 °C using goat anti-rabbit Fab IgG fragments followed by the second primary antibody. Immunolabeled sections were examined on a Nikon Microphot FXL epifluorescent microscope equipped with Olympus digital camera or Olympus Fluoview 500 confocal microscope using 20×, 40×, 60×, or 100× oil objectives. Post-acquisition analysis and quantification of fluorescence intensities was performed using Metamorph software (Molecular Devices). Images from immunolabeled sections taken at 60× magnification were used for fluorescence intensity quantification as described previously (6). CFTR fluorescence was determined using images taken from sections containing fields with an average of 14–17 crypts, and alkaline phosphatase fluorescence was determined in villus sections (five fields). The data were collected following subtraction of fluorescence values for secondary antibody alone from five different fields each from random immunolabeled sections of Dab2 control and KO jejunum. The data represent the average pixel intensity with S.E. The significance was measured by Student's *t* test.

Immunofluorescence Microscopy of Cells—Confluent monolayers of polarized CaCo-2_{BB}e cells were fixed in 2% paraformaldehyde-PBS for 10 min at room temperature. The cells were permeabilized with 0.1% Triton X-100 in PBS for 10 min followed by incubation with 0.5% bovine serum albumin and 0.15% glycine in PBS for 45 min to block nonspecific binding. The primary antibodies were prepared in blocking solution containing 0.1% Triton X-100 and applied overnight at 4 °C. The cells were washed and incubated with the appropriate secondary antibodies for 1 h at room temperature, and nuclear stain (Draq 5; Biostatus) was applied. The filters were mounted with Slow Fade medium and/or embedded in Tissue-Tek O.C. T medium and sectioned in the vertical plane prior to examination by confocal microscopy.

Immunohistochemistry—Immunohistochemistry was performed as described (22) using a Vectastain Elite ABC kit (Vector Laboratories, Inc.). Paraffin-embedded tissue sections from Dab2 control and knock-out mice were immunolabeled following the manufacturer's instructions and antigen retrieval as described above. The sections were incubated with primary antibodies overnight at 4 °C. Following immunolabeling, the sections were counterstained with Meyer's Hematoxylin solution and mounted with Permount, and the sections were examined on an Olympus Provis microscope equipped with digital camera.

Immunoprecipitation and Western Blotting—The cells or mucosal scrapings were lysed in TGH buffer (1% Triton X-100, 25 mM Hepes, and 10% glycerol, pH 7.4) containing protease inhibitors followed by centrifugation at 15,000 rpm for 15 min at 4 °C. The supernatants from mucosal scrapings of rat jejunum and CaCo-2_{BB}e cells were precleared by incubation with 25 μl of protein A beads for 20 min on ice. The samples were centrifuged for 30 s at maximum speed, and supernatants were incubated with 1 μg of specific antibody (AME 4991, anti-α-AP-2, and anti-myosin VI) on ice for 90 min, followed by 20 μl of 50% protein A beads, and the samples were rocked for one h at 4 °C. After centrifugation (14,000 rpm), protein-antibody-bead complexes were washed with 1× radioimmune precipitation assay (500 mM Hepes, 150 mM NaCl, 1% Triton X-100, and 1 mM EDTA) buffer, and samples were eluted with 5× SDS sample buffer before analysis by Western blot (6, 7).

GST Constructs and Mutagenesis—GST, GST-Dab2 (1–205), (1–368), (601–768), and α_c AP-2 appendage fusion proteins were provided by Dr. Linton Traub (University of Pittsburgh). GST-Dab2 (1–368) served as the template for introduction of mutations. Mutagenesis of this construct at positions amino acids 293–295 and 298–300 of Dab2 (23) was performed using QuikChange protocol (Stratagene) with the following primer: 5′-CCCCTAACCCTGCTCCTGCCCGTGATGCTCCCGCTGCACAGCCAG-3′. All of the constructs and mutations were verified by sequencing.

Protein and Peptide Preparation—Expression and purification of GST fusion proteins were performed as described (23, 24). GST and the various GST fusion proteins produced in *Escherichia coli* BL21 cells were grown in 20 ml of LB Broth (Invitrogen) plus ampicillin (200 μg) (Fisher) overnight at 37 °C with constant shaking to create a starter culture. From the starter culture, the bacteria was diluted 1:50 in the LB broth, grown to an A_{600} of 0.6 at 37 °C with constant shaking, and induced with isopropyl-1-thio-β-D-galactopyranoside (100 μM). After 3–5 h with constant shaking at room temperature or A_{600} of 1.3–1.4, the bacteria were recovered by centrifugation at 15,000 rpm (JA-14 rotor) at 4 °C for 15 min, and the pellets were stored at −80 °C. The pellets were resuspended in bacterial lysis sonification buffer (50 mM Tris-HCl, pH 8.0, 300 mM NaCl, 0.2% Triton X-100, and 10 mM 2-mercaptoethanol) containing 100 mM phenylmethylsulfonyl fluoride, sonicated, and centrifuged at 14,000 rpm (JA-20 rotor) at 4 °C for 15 min. The supernatants were incubated with 1 ml of 75% glutathione-Sepharose 4B bead slurry (Amersham Biosciences). The beads were col-

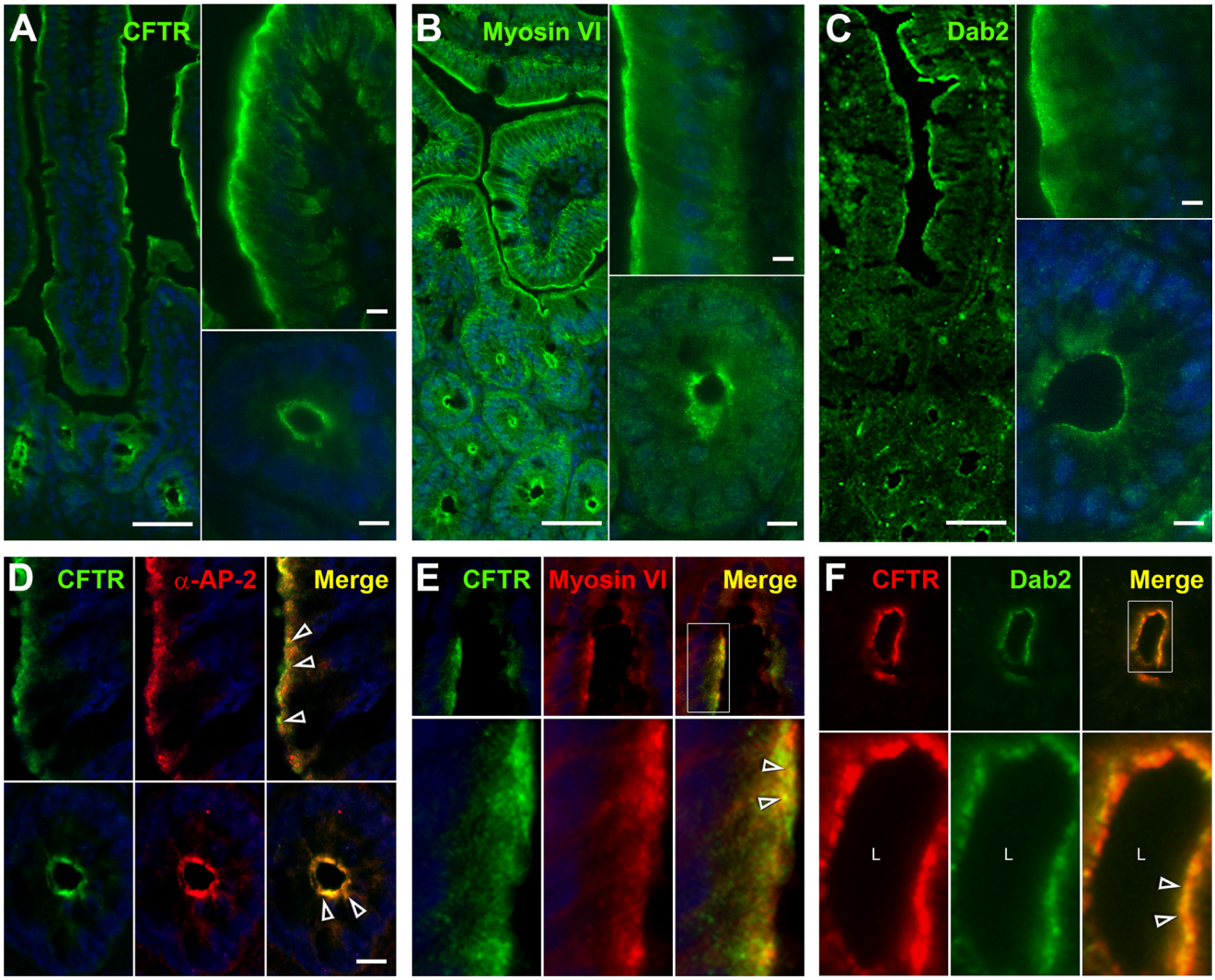

FIGURE 1. **Distribution of CFTR relative to α-AP-2, myosin VI, and Dab2 in the small intestine.** Cryostat sections of mouse and rat jejunum were labeled with anti-CFTR, myosin VI, Dab2, and α-AP-2 antibodies and examined by confocal microscopy. Low (*A–C*, *left panels*) and high magnification (*A–C*, *upper right panels and lower right panels*) images of villus (*A–C*, *upper right panels*) and crypt (*A–C*, *lower right panels*) show the distribution of CFTR (*A*, *green*), myosin VI (*B*, *green*), and Dab2 (*C*, *green*). *Scale bar*, 100 μm. *D*, high magnification image of mouse villus and crypt section shows the localization of CFTR (*green*) relative to α-AP-2 (*red*) and merged image (*yellow*, *open arrowheads*). *E*, higher magnification of a crypt in mouse jejunum shows the distribution of CFTR (*green*), myosin VI (*red*), and merged image (*yellow*, *open arrowheads*). *F*, higher magnification of a crypt in rat jejunum shows the distribution of CFTR (*red*), Dab2 (*green*), and merged image (*yellow*, *open arrowheads*). The nuclei are stained *blue*. *Scale bar*, 10 μm; *L*, lumen.

lected by centrifugation at 500 × *g* for 5 min at 4 °C. GST fusion proteins bound to beads were washed in PBS, and the proteins were eluted with glutathione elution buffer (25 mM Tris-HCl, pH 8.0, 200 mM NaCl, and 10 mM glutathione) with 1 mM dithiothreitol on ice. Eluted fusion proteins were pooled, dialyzed in PBS, and stored at −80 °C prior to performing binding assays.

Binding Assays—Binding assays were preformed as described (11). Polarized CaCo-2_{BB}e cells or rat jejunum mucosal scrapings were washed with PBS. The cells were lysed in TGH buffer containing protease inhibitors. GST and GST fusion proteins (200–500 μg) were bound to 60 μl of 50% glutathione-Sepharose 4B bead slurry at 4 °C for 1 h while continuously rotating. After 1 h, cell supernatants (300 μl, 6.06 μg/μl) were added, and tubes were incubated at 4 °C overnight with continuously rotating. The Sepharose beads with bound complexes of proteins and supernatants were centrifuged at 10,000 rpm at 4 °C for 1 min, supernatants were discarded, and pellets were washed three times with cold PBS. The pellets were resuspended to a final volume of 90 μl with 5× SDS sample buffer and one-fourth of each pellet was resolved by SDS-PAGE gels and stained with Coomassie Blue (Bio-Rad) or analyzed by Western blot.

siRNA Transfection and Endocytosis Assays—HEK 293 cells were plated onto 35-mm dishes (BD Falcon) and allowed to propagate in medium without hygromycin for 24 h prior to transfection. The cells were transfected at 70% confluency using α-AP-2 siRNA and Lipofectamine™ 2000 reagent according to the manufacturer's instructions. After 24 h, the culture medium was changed. The cells were lysed and analyzed for α-AP-2 expression by Western blot at 72 h. Endocytosis assays were performed in cells following silencing of α-AP-2 expression and controls included nontransfected or scrambled siRNA transfected cells. The cell surface biotinylation and endocytosis assays were performed as previously

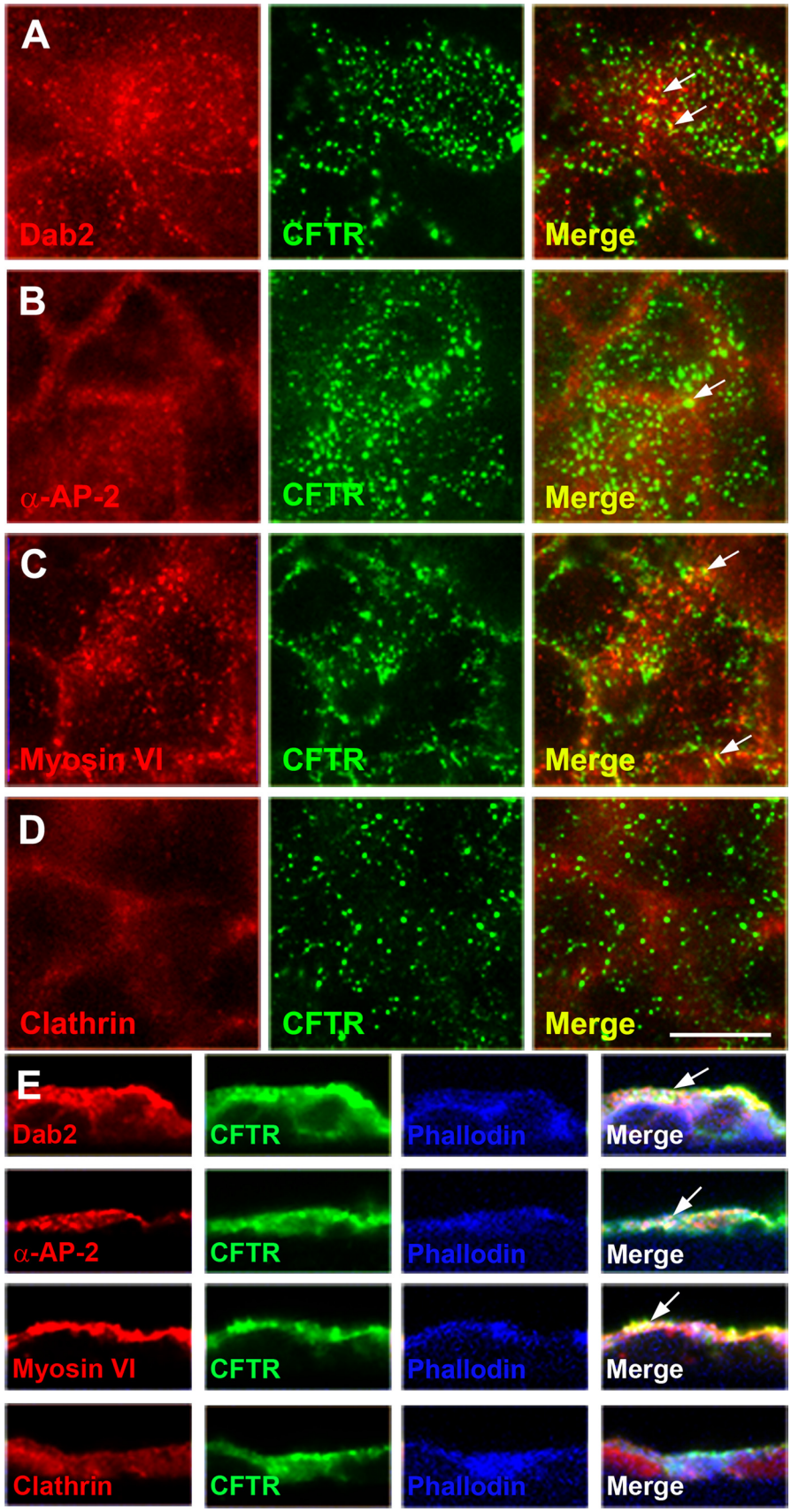

FIGURE 2. **Localization of endogenous Dab2, α-AP-2, myosin VI, clathrin, and CFTR in confluent monolayers of polarized CaCo-2$_{BB}$e cells.** *A–D*, enface images taken at the level of the brush border. Dab2 (*A*, *left panel*, *red*), α-AP-2 (*B*, *left panel*, *red*), myosin VI (*C*, *left panel*, *red*), clathrin (*D*, *left panel*, *red*), and CFTR (*A–D*, *middle panels*, *green*). The merged images are shown (*A–D*, *right panels*). *E*, images of XZ vertical sections of *A–D*. The *arrows* indicate co-localization (*white*). *Scale bar*, 10 μm.

described (25). The samples were analyzed by Western blot, and CFTR was quantified using Bio-Rad Fluor S-Multimager and Quantity One Image Analysis Software. The data are expressed as the means ± S.E. ($n > 3$). Significant differences were determined using a two-tailed Student's *t* test (the *p* values of <0.05 was considered significant).

RESULTS

Localization of Endogenous Dab2 and α-AP-2 Relative to CFTR and Myosin VI in the Intestine—CFTR is present on microvillar membranes, clathrin-coated pits, and vesicles in enterocytes of the small intestine and co-localizes with myosin VI in the apical domain (6, 15). Dab2 is the binding partner for myosin VI and α-AP-2, but its expression and distribution has not been established in the intestine. Localization of Dab2 and α-AP-2 in the apical domain of the intestine provides strong support for a physiologic interaction with CFTR and myosin VI. Because Dab2 also binds to the α-AP-2 appendage, we examined the distribution of Dab2, and α-AP-2 relative to CFTR and myosin VI in sections of small intestine using indirect immunofluorescence microscopy. CFTR and myosin VI were observed in their predicted location in the apical domain of enterocytes (Fig. 1, *A* and *B*) (6). Dab2 was also distributed in the apical domain of crypt and villus cells and co-localized with CFTR, but Dab2 staining was observed in a location beneath CFTR (Fig. 1, *C* and *F*). Anti-α-AP-2 specific antibodies also confirm CFTR co-localization with α-AP-2 in the apical domain of villus and crypt enterocytes (Fig. 1*D*).

Distribution of Endogenous CFTR and Endocytic Proteins in Polarized CaCo-2_{BB}e—To investigate the interactions of Dab2-α-AP-2 and endogenous CFTR in the intestine, we employed polarized CaCo-2_{BB}e cells grown on permeable filters. The $_{BB}$e subclone of CaCo-2 cells consists of a homogeneous population of differentiated enterocytes devoid of goblet cells. This polarized cell model was previously characterized for the study of brush border assembly and intestinal myosins including myosin VI but has not been employed in CFTR studies (26, 27). The distribution of endogenous CFTR, clathrin, myosin VI, Dab2, and α-AP-2 in CaCo-2_{BB}e cells is shown in Fig. 2. Consistent with its distribution in the native intestine, CFTR is abundant in the brush border and in subapical structures beneath the apical membrane. Dab2-containing structures co-localize with CFTR in the apical domain (Fig. 2, *A* and *E*). α-AP-2 is also in the apical domain and is observed in CFTR-containing structures (Fig. 2, *B* and *E*). Myosin VI stains intensely in the apical domain (Fig. 2*C*) and co-localizes with CFTR-containing structures beneath the plasma membrane (Fig. 2*E*), consistent with its localization in intestinal tissues. Clathrin predominantly stains structures beneath CFTR on the plasma membrane (Fig. 2*D*), but a few clathrin containing structures were also positive for CFTR (Fig. 2*E*).

CFTR Is in a Complex with α-AP-2, Myosin VI, and Dab2 in the Apical Domain of the Intestine—To determine whether CFTR physiologically interacts with Dab2, α-AP-2, and myosin VI *in vivo*, we immunoprecipitated CFTR from rat small intestine and polarized CaCo-2_{BB}e cells and analyzed the samples by Western blot. Western blot analysis (20 μg of protein) of polarized CaCo-2_{BB}e cells revealed endogenous expression of CFTR, Dab2, α-AP-2, myosin VI, and clathrin (Fig. 3*A*). CaCo-2_{BB}e cell lysates were immunoprecipitated with anti-CFTR or non-specific antibody and immunoblotted with anti-myosin VI, anti-Dab2 or anti-α-AP-2 antibodies. Intestinal CFTR derived from endogenously expressing CaCo-2_{BB}e cells (Fig. 3*B*) and rat intestine (Fig. 3*C*) co-immunoprecipitated with myosin VI, α-AP-2, and Dab2.

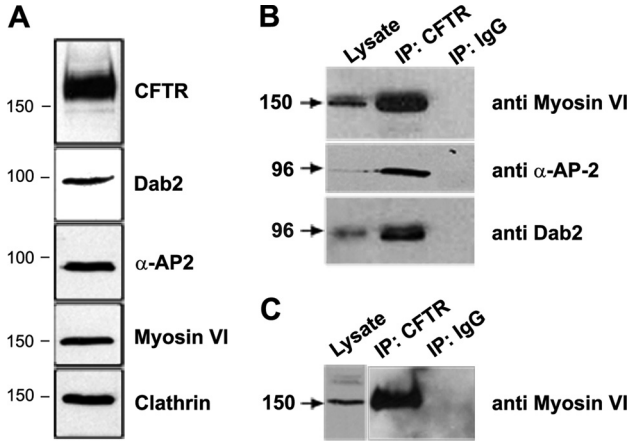

FIGURE 3. **Western blot analysis and co-immunoprecipitation of endogenous CFTR with endocytic adaptor proteins in polarized CaCo-2_{BB}e cells and rat jejunum.** *A*, Western blot analysis of CFTR, Dab2, α-AP-2, myosin VI and clathrin in polarized CaCo-2_{BB}e cells. Equivalent protein loads (20 μg) from cell lysates were resolved by SDS-PAGE, and proteins were detected by immunoblot. *B* and *C*, CFTR or control IgG were immunoprecipitated (*IP*) from cell lysates prepared from polarized CaCo-2_{BB}e cells (*B*) or rat jejunum and immunoprecipitates were analyzed by Western blot to detect myosin VI, α-AP-2, and Dab2 (*C*).

Dab2 Regulates the Abundance of Apical CFTR in the Intestine—Absence of myosin VI leads to increased surface CFTR and defective apical endocytosis in the intestine. Because Dab2 is the binding partner for myosin VI and associates with CFTR in the intestine, we examined the distribution of CFTR in the small intestine of Dab2 knock-out mice. These animals lack Dab2 gene expression in most cells, including enterocytes of the intestine (Fig. 4, *A* and *B*) (22, 28). Immunofluorescence labeling for CFTR revealed the typical apical domain staining in both control and Dab2 knock-out sections (Fig. 4, *C* and *D*), but higher levels of CFTR were observed in Dab2 knock-out tissues (Fig. 4, *D* and *E*), suggesting that Dab2 regulates surface CFTR. Quantification of CFTR labeling in sections was performed using fluorescence intensities and a control marker, the brush border alkaline phosphatase, an enzyme that hydrolyzes monophosphate esters and is not regulated by clathrin-mediated endocytosis. The observed increase in surface CFTR in Dab2 KO tissues was not as prominent compared with CFTR levels in the myosin VI mutant intestine (6). The mild increase of CFTR is consistent with the transient nature of interactions between endocytic adaptors and surface receptors and/or an indirect role for Dab2 in myosin VI-dependent endocytosis of CFTR. The distribution and abundance of alkaline phosphatase in Dab2 knock-out and control sections remained unchanged (Fig. 4*E*).

CFTR Binds to the AP-2 α Appendage but Not Dab2 in the Intestine—Dab2 binds to a DPF motif within its central region to the AP-2 α appendage (17, 23), to myosin VI within its C

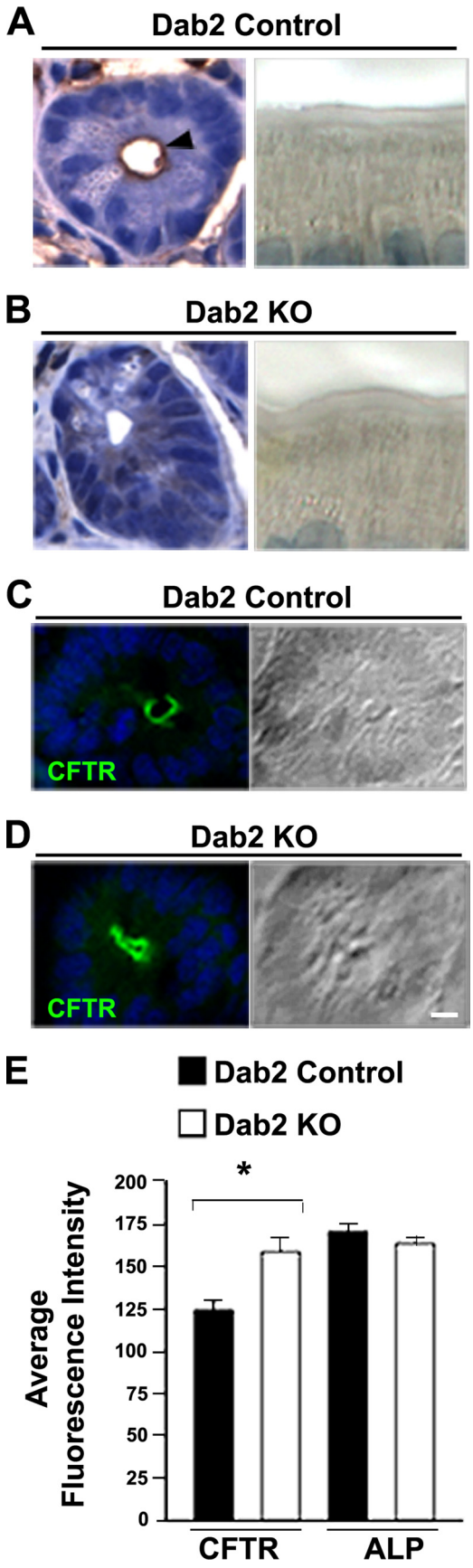

FIGURE 4. **Distribution of Dab2 and CFTR in jejunum sections from Dab2 control and knock-out mice.** *A* and *B*, immunohistochemical staining of Dab2 in control (*A*) and knock-out (*B*) jejunum. Dab2 staining (*arrowhead*) in control (*A*) and KO (*B*) crypt is shown. The corresponding panels on the *right* show staining in the absence of primary antibody. *C* and *D*, cryostat sections were labeled with CFTR antibody and examined by confocal microscopy. Apical distribution of CFTR (*C* and *D*, *green*) in crypt from Dab2 control (*C*) and KO (*D*) jejunum. Hoechst stain labels nuclei *blue*. *Right panels*, differential interference contrast images from corresponding labeled sections. *E*, quantification of fluorescence intensities (*FI*) for CFTR and alkaline phosphatase (*ALP*). The data are shown as the means ± S.E. *, $p < 0.05$ ($n > 10$ sections from each group). *Scale bar*, 10 μm.

terminus (29), and to members of the LDLR family at the N terminus at its PTB (F*X*NP*XY*) domain (amino acids 1–205) (Fig. 5, *A* and *B*) (19). Because Dab2 binds α-AP-2 and co-immunoprecipitates with CFTR in the intestine, we used GST-Dab2 and α-AP-2 fusion proteins in pulldown assays to examine whether Dab2 or α-AP-2 binds to CFTR in the native intestine. GST-Dab2 bound directly to the C terminus of myosin VI *in vivo* in the intestine (Fig. 5, *C* and *F*). Neither GST-Dab2 PTB domain (1–205) nor GST-Dab2 (1–368) that includes the DPF domain bound to CFTR (Fig. 5, *D*, *E*, and *G*). GST-α-AP-2 appendage bound to CFTR (Fig. 5, *E* and *G*). GST-Dab2 (1–368) bound to α-AP-2, but site-directed mutagenesis of the DPF motif failed to eliminate its binding *in vivo* (Fig. 5*H*). These data indicate that in the intestine CFTR interacts with Dab2 indirectly through its interaction with the α-AP-2 appendage and further support the observations as shown in Fig. 4 of a mild increase in apical CFTR in the Dab2 knock-out intestine.

Endocytosis of CFTR Requires α-AP-2—To determine whether α-AP-2 directly regulated CFTR internalization, surface biotinylation approaches were employed to examine CFTR endocytosis in CFTR-expressing HEK cells following siRNA knockdown of α-AP-2 (Fig. 6). Introduction of siRNA reduced α-AP-2 expression by 64% in CFTR-expressing cells. Internalization of CFTR from the plasma membrane was determined at 1 and 5 min to ensure completion of early endocytosis and engagement of endocytic adaptors. In α-AP-2 knockdown cells, endocytosed CFTR from the plasma membrane was reduced from 11 to 3% at 1 min and from 37 to 17% at 5 min (Fig. 6, *B* and *C*). These results indicate that endocytosis of CFTR requires α-AP-2 and are consistent with the results of the GST pulldown assays indicating that α-AP-2 is a binding partner for CFTR.

α-AP-2 Is Localized to the Terminal Web Region and Not Redistributed in Dab2 Knock-out or Myo 6$^{(sv/sv)}$ Enterocytes—GST pulldown assays indicated that CFTR binds to α-AP-2. Because α-AP-2 engages Dab2 and links it to myosin VI, we immunolabeled sections of small intestine from Dab2 and Myo 6$^{(sv/sv)}$ mutant mice to determine whether absence of myosin VI or Dab2 *in vivo* alters the localization of α-AP-2 in enterocytes. Immunofluorescence labeling for α-AP-2 in villus sections from myosin VI heterozygote Myo 6$^{(sv/wt)}$ (supplemental Fig. S1*A*) or Myo 6$^{(sv/sv)}$ animals (supplemental Fig. 1*B*) revealed its enrichment in the terminal web region just below the brush border. In Dab2 KO (supplemental Fig. 1*D*) and control sections (supplemental Fig. S1*C*), the distribution of α-AP-2 was similarly enriched in the terminal web and appeared to be unaltered in the absence of Dab2 or myosin VI.

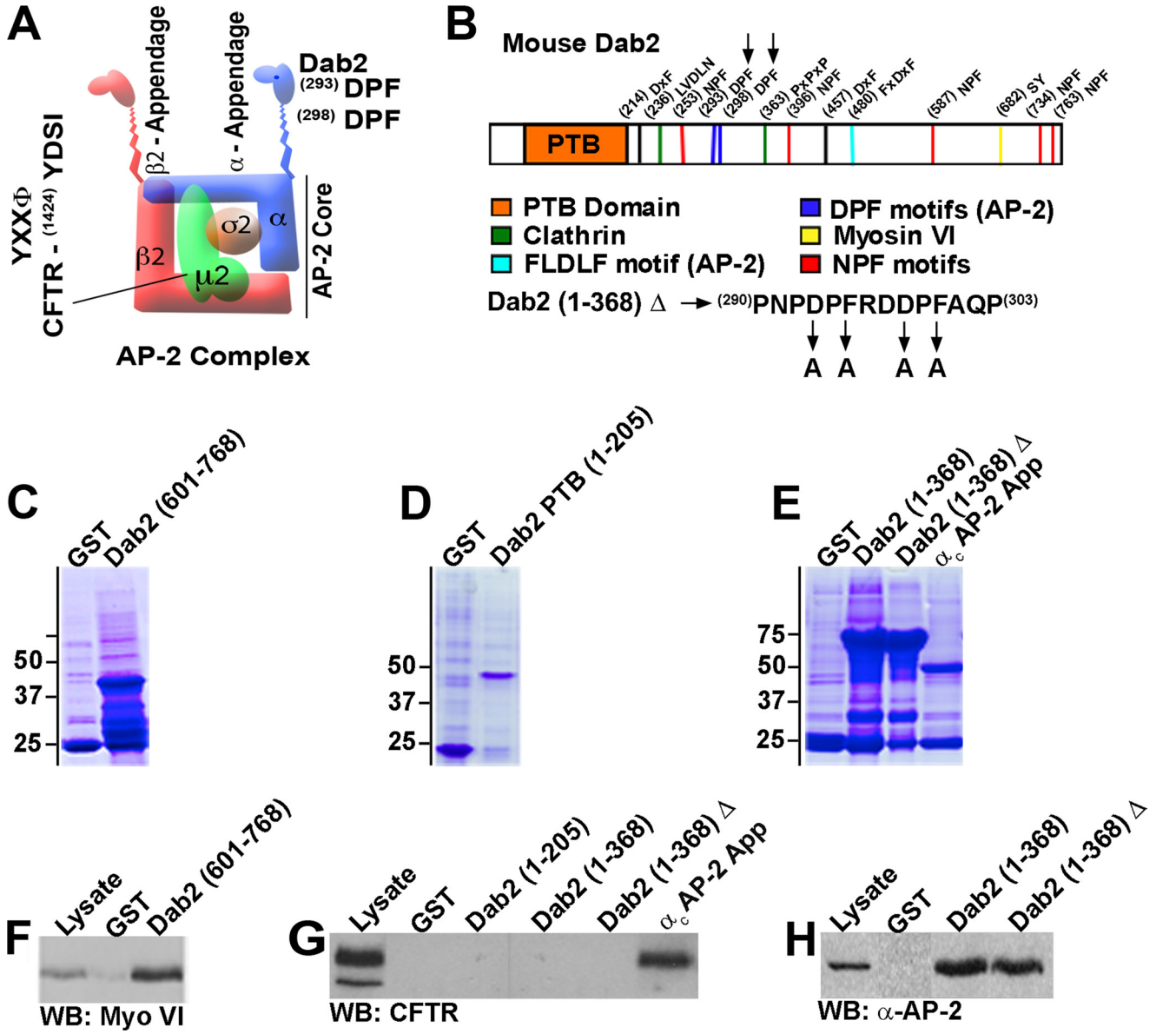

FIGURE 5. **GST binding assays in rat intestine.** *A*, schematic diagram of AP-2 complex indicates the known site of CFTR engagement to the μ2 subunit and binding site for Dab2 (DPF) to the α ear appendage. *B*, schematic map of binding domains in mouse Dab-2. Sequence of amino acids 290–303 of Dab2 indicates mutagenesis sites (*black arrows*). GST or GST-Dab2 (601–678), Dab2 (1–205), Dab2 (1–368), Dab2 (1–368Δ), and GST-α_c-adaptin appendage (250–500 μg) were bound to 60 μl of glutathione-Sepharose bead slurry and incubated with 6.06 μg/ml rat jejunum lysate overnight at 4 °C. The samples were centrifuged to recover the pellet. 20 μg of rat jejunum lysate and one-fourth of each pellet were resolved on SDS-PAGE gels and stained with Coomassie Blue (*C–E*) or transferred to polyvinylidene difluoride nitrocellulose (*F–H*). *F*, Western blots (*WB*) show binding of GST-Dab2 (601–768) to myosin VI. *G*, no binding to CFTR is detected with GST-Dab2 1–205 (PTB domain), Dab2 (1–368), or Dab2 (1–368Δ), but GST-α_c-adaptin appendage binds robustly to CFTR. *H*, GST-Dab2 (1–368) and Dab2 (1–368Δ) binding to α-AP-2. The blots were probed with anti-myosin VI, α-AP-2, and CFTR antibodies. The positions of the molecular mass standards (kDa) are indicated.

Dab2 Accumulates in the Terminal Web of Myo 6$^{(sv/sv)}$ Enterocytes—Previous Western blot analyses of intestinal epithelium from Myo 6$^{(sv/sv)}$ mice indicated that the absence of myosin VI did not alter Dab2 protein expression (6). The specific steps where myosin VI exerts its action in directing endocytosis is unknown. However, it has been suggested that myosin VI may move and position Dab2 at sites of clathrin-mediated endocytosis (18). To determine whether myosin VI plays a role in localizing Dab2 in enterocytes, we immunolabeled sections of jejunum from Myo 6$^{(sv/sv)}$ and heterozygote control Myo 6$^{(sv/wt)}$ littermates. Dab2 localized to the terminal web region just below the brush border in heterozygote Myo 6$^{(sv/wt)}$ enterocytes (Fig. 7, A), consistent with its distribution in other polarized tissues such as the kidney cortex (28). In Myo 6$^{(sv/sv)}$ enterocytes (Fig. 7*B*), Dab2 accumulated in the terminal web. Staining for Dab2 in Myo 6$^{(sv/sv)}$ co-localized with F-actin in the lower portions of the microvilli (Fig. 7*B*, *white arrowheads*) but not in Myo 6$^{(sv/wt)}$ enterocytes. The accumulation of Dab-2 in the terminal web of Myo 6$^{(sv/sv)}$ enterocytes correlated strongly with prominent involution and an upward redistribution of the intermicrovillar membranes toward the microvillar tips that was observed by ultrastructural TEM examination (Fig. 7, *C* and *D*). The upward migration of the microvillar plasma membrane in Myo 6$^{(sv/sv)}$ enterocytes resulted in an expan-

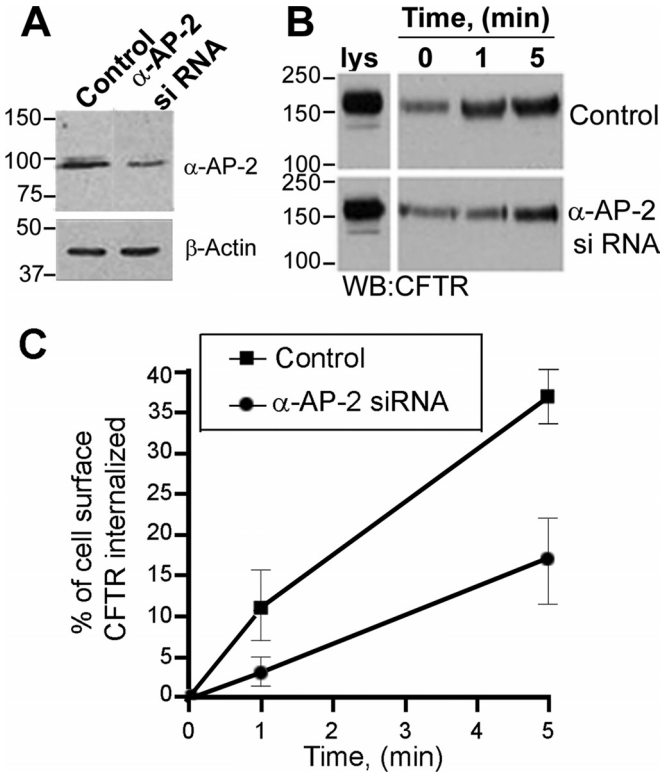

FIGURE 6. **siRNA knockdown of α-AP-2 reduces CFTR endocytosis.** *A*, HEK 293 cells expressing CFTR were incubated overnight in Dulbecco's modified Eagle's medium with 10% fetal bovine serum and allowed to grow to 70% confluency. The cells were transfected with α-AP-2 or scrambled siRNA and analyzed by Western blot at 72 h to detect α-AP-2 and β-actin (*A*). *B*, cell surface proteins were labeled using NHS SS-biotin and allowed to internalize for 1 and 5 min at 37 °C. Following MESNA treatment, the cells were lysed, surface biotinylated proteins were bound to streptavidin-agarose beads, and CFTR was detected by Western blot. *C*, the percentage of cell surface CFTR internalized over time is shown. The data are expressed as the means ± S.E. ($n > 3$).

sion of the terminal web and shorter microvilli. These observations are consistent with a physiologic role for myosin VI in positioning the intermicrovillar membrane and Dab2 within the clathrin coat machinery, membrane invagination, and formation of coated pits to begin apical endocytosis at the base of the microvilli.

DISCUSSION

Endocytic recycling is a physiologically important mechanism that regulates CFTR surface expression and anion transport *in vivo*, contributes to intestinal disease, and is critical to enterocyte biology (6, 7, 9, 10). Here we sought to understand the physiologic binding partners and mechanisms that regulate apical endocytosis of CFTR in the intestine. In a previous study we demonstrated that myosin VI, a minus end-directed actin motor, played a crucial role in regulating CFTR surface expression, apical endocytosis, and ion transport in the small intestine (6). But the specific endocytic binding partner that links CFTR to myosin VI was unknown. Moreover, although myosin VI is widely recognized as a key regulator of clathrin-mediated endocytosis, the specific site or steps where it exerts its function in regulating endocytosis is unknown. In this study, we employed intestinal tissues from Snell's Waltzer Myo $6^{(sv/sv)}$ and heterozygote Myo $6^{(sv/wt)}$ control littermates, Dab2 KO and control mice, polarized CaCo-2_{BB}e cells, and rat intestinal epithelium to examine the physiologic endocytic adaptors involved in myosin VI-dependent endocytosis of CFTR. We also sought to understand the sites where myosin VI exerts its activity in regulating apical endocytosis in the enterocyte.

Localization studies in native small intestinal epithelium identified the endocytic adaptors α-AP-2, and Dab2 in the apical domain of enterocytes in a distribution that overlapped myosin VI and CFTR. Western blots confirmed endogenous expression of the endocytic proteins in rat intestine, and co-immunoprecipitation experiments indicated that α-AP-2, Dab2, myosin VI, and CFTR were in a complex in the apical domain of the intestine. CFTR was previously identified in a complex with α-AP-2 in clathrin-coated vesicles from cultured endogenous CFTR-expressing intestinal cells (30, 31) and with Dab2 and myosin VI in airway epithelial cells (32). Furthermore, binding of the C terminus of CFTR to α-AP-2 was also demonstrated, but the precise site of binding within the AP-2 core subunit or ear appendage was not determined (31). Similarly, except for its existence in a complex in airway cells with CFTR, nothing was known regarding the relationship of Dab2/myosin VI to CFTR. The availability of intestinal tissues from Dab2 knock-out mice allowed us to directly examine whether the lack of Dab2 *in vivo* modulates CFTR abundance on the apical membrane. We observed a mild but specific accumulation of CFTR in the apical domain in sections of Dab2 KO intestines when measured relative to the brush border marker alkaline phosphatase. Whether CFTR increased in the apical membranes of enterocytes in the absence of Dab2 *in vivo* because of a direct interaction was unclear. Unlike members of the LDL receptor family that undergo myosin VI-dependent endocytosis by recognizing and binding to a PTB domain within Dab2, CFTR lacks a PTB domain in its sequence. However, Dab2 binds within its central region at a DPF domain to the ear appendage of α-AP-2.

The results of our pulldown assays using cytosol from rat intestine, GST-Dab2, GST-α-AP-2 appendage, and mutant fusion proteins confirmed that myosin VI binds to Dab2 within the C terminus. Site-directed mutagenesis of amino acids 293–298 (DPF) within the central region of Dab2, GST (1–368Δ), where it binds to the α-AP-2 appendage slightly reduced but did not abrogate its binding. These findings are consistent with the notion that DPF may not be necessary for Dab2 binding to the α-AP-2 appendage (19). No binding of GST-Dab2 PTB domain (1–205), GST (1–368), or GST (1–368Δ) to CFTR was detected in the intestine, consistent with the lack of a PTB domain in CFTR (Fig. 5). However, we identified robust binding of CFTR to GST-α-AP-2 appendage. Endocytosis assays in cells following siRNA knockdown of α-AP-2 confirmed that CFTR internalization was markedly impaired, further supporting the GST binding studies. Together, the findings here suggest that myosin VI-dependent endocytosis of CFTR requires direct binding of CFTR to α-AP-2 rather than Dab2. Because Dab2 binds to α-AP-2 and myosin VI, the absence of Dab2 *in vivo* could lead to a mild increase of apical CFTR as observed in Dab2 KO enterocytes.

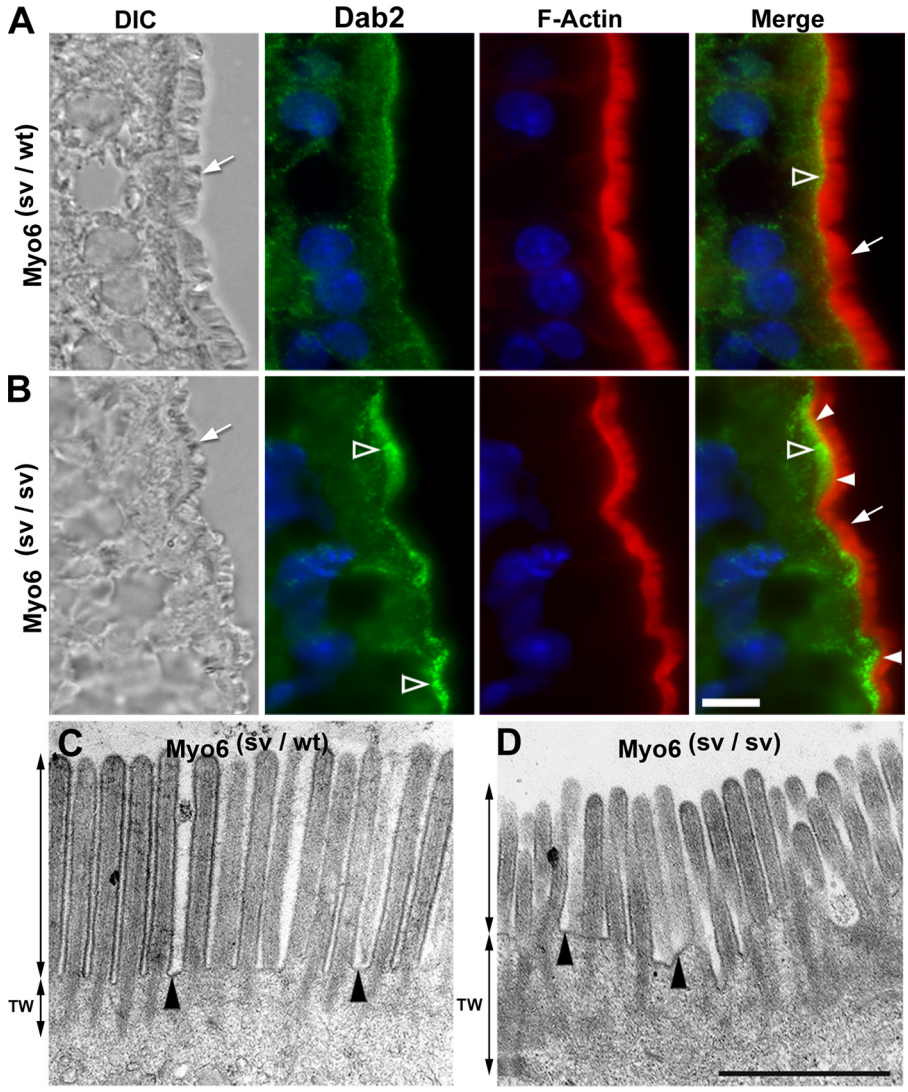

FIGURE 7. **Immunofluorescence distribution of Dab2 and TEM of the brush border domain from heterozygote Myo 6$^{(sv/wt)}$ and Myo 6$^{(sv/sv)}$ knock-out mice.** Cryostat sections were doubled labeled with anti-Dab2 antibodies, and F-actin was detected with rhodamine phalloidin. *A* and *B*, *left* to *right*, differential interference contrast (*DIC*), Dab2 (*green*), F-actin (*red*), and merged images from heterozygote Myo 6$^{(sv/wt)}$ (*A*) and Myo 6$^{(sv/sv)}$ (*B*) KO sections. Rhodamine phalloidin (*red*) identifies microvilli (*white arrows*). Dab2 staining in the terminal web (*open arrowheads*) is indicated. In differential interference contrast images, the microvilli appear shorter in Myo 6$^{(sv/sv)}$ (*B*) compared with heterozygote Myo 6$^{(sv/wt)}$ (*A*) terminal web region accumulation of Dab2 staining (*open arrowheads*) and co-localization of Dab-2 with Phalloidin (*white arrowheads*) in the lower portions of the microvilli. Hoechst stain labels the nuclei *blue*. *Scale bar*, 10 μm. *C* and *D*, TEM of the brush border domain of Myo 6$^{(sv/wt)}$ (*C*) and Myo 6$^{(sv/sv)}$ enterocytes (*D*). In Myo 6$^{(sv/wt)}$ the intermicrovillar membrane of enterocytes is perpendicular to the microvilli (*C*, *black arrowheads*). In contrast, the intermicrovillar domain is uneven in Myo 6$^{(sv/sv)}$ (*D*, *black arrowheads*), resulting in a highly variable microvillar length and increased intervillar membrane surface area relative to the heterozygous control that expands the terminal web (*TW*) region as shown. *Scale bar*, 1 μm.

AP-2 selects surface membrane proteins for endocytosis by recognizing specific signals in their cytoplasmic tails. Tyrosine and di-leucine motifs endocytic have been best characterized, and both are identified in CFTR (33, 34). Cross-linking experiments revealed direct binding of a tyrosine internalization motif in the C terminus of CFTR to the AP-2 μ2 subunit, and overexpression of dominant negative μ2 reduced CFTR internalization in a heterologous expression model (35). The findings here would support involvement of a di-leucine motif in engaging CFTR to AP-2 α appendage to direct myosin VI-dependent endocytosis in the intestine.

The localization of α-AP-2 and Dab2 in the terminal web beneath the brush border is consistent with their roles as adaptors in clathrin coat assembly and myosin VI-dependent endocytosis of CFTR or other apical membrane receptors. We could not appreciate changes in steady state distribution of α-AP-2 in the terminal web of Dab2 KO tissues by light microcopy. The abnormal accumulation of Dab2 in the terminal web of Myo 6$^{(sv/sv)}$ enterocytes and its overlap with the lower portions of the microvilli (Fig. 7) was intriguing and suggested that the absence of myosin VI in enterocytes may affect Dab2-dependent assembly of clathrin coat, the terminal web, the intermicrovillar domain, and the ability of the membrane to invaginate to create a coated pit.

Ultrastructural examination (Fig. 7) provided some explanations for the observed accumulation of Dab2 in Myo 6$^{(sv/sv)}$ enterocytes and the co-localization of Dab2 in the microvilli. The highly variable microvillar length and increased intervillar membrane surface area in Myo 6$^{(sv/sv)}$ enterocytes resulted in an expansion of the terminal web region (Fig. 7*D*) with accumulation of Dab2 and its apparent extension up into the microvilli (Fig. 7*B*) in the absence of myosin VI. Immunolocalization did not identify labeling for either Dab2 or α-AP-2 in the brush border microvillar membranes (except for the overlap of Dab2 at the base of Myo 6$^{(sv/sv)}$ microvilli) and therefore do not support a role for myosin VI in moving adaptor complexes down the microvilli. Consistent with this finding is the recent observation that the clathrin receptor megalin is also properly localized to the intermicrovillar domain in the proximal tubule of Myo 6$^{(sv/sv)}$ mice (36). The findings here support a role for myosin VI in 1) securing the intermicrovillar membrane in its normal orientation to promote invagination and coated pit formation and 2) moving the coated vesicle and adaptors away from the plasma membrane to allow internalization of receptors following scission of the invagination. A model depicting this pathway for myosin VI-dependent endocytosis of CFTR in the intestine is shown in Fig. 8. The findings reported here provide a more detailed understanding of the mechanisms

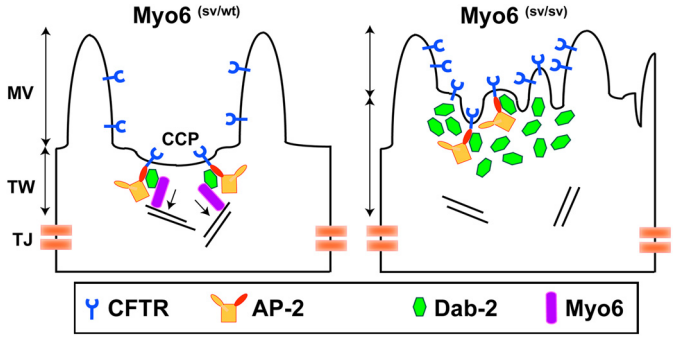

FIGURE 8. **Proposed model depicting endocytic adaptors involved in myosin VI-dependent endocytosis of CFTR and role of myosin VI in apical endocytosis.** *Left panel*, in the heterozygote Myo $6^{(sv/wt)}$ or normal enterocyte CFTR is in the apical microvillar membrane and coated pits. AP-2 is recruited to the cytoplasmic surface of the intermicrovillar membrane where it interacts with CFTR via the α-subunit. Dab-2 binds to the α-AP-2 appendage and links CFTR to myosin VI that is in the terminal web region. *Right panel*, in Myo $6^{(sv/sv)}$ KO enterocytes, CFTR accumulates on the apical microvillar membrane, and endocytosis is impaired. In the absence of myosin VI stabilization of the intermicrovillar membrane is lost, resulting in upward migration of the membrane, and shorter microvilli with variable lengths and an expanded terminal web. The absence of myosin VI results in the lack of tension necessary for membrane invagination, defective assembly of the coated pit, and accumulation of Dab2 in the terminal web. Myosin VI may also help to move the coated vesicle and adaptors away from the plasma membrane for internalization of CFTR. *MV*, microvilli; *TW*, terminal web; *TJ*, tight junction; *CCP*, clathrin-coated pit.

underlying our previous observations of marked accumulation of surface CFTR and defective early endocytosis observed in Myo $6^{(sv/sv)}$ enterocytes.

Acknowledgments—We thank Sean Alber and Christine Goldbach of the Center for Biologic Imaging (University of Pittsburgh) for excellent technical assistance and Dr. Linton Traub (University of Pittsburgh School of Medicine) for providing GST constructs and instruction in GST binding assays. We are also grateful to Dr. Jonathan Cooper (Fred Hutchinson Cancer Research Center, Seattle, WA) for providing Dab2 mouse tissues.

REFERENCES

1. Trier, J. L. M. J. (1994) in *Physiology of the Gastrointestinal Tract* (Johnson, L. R., ed) 3rd Ed., Raven Press, New York
2. Ameen, N., Alexis, J., and Salas, P. (2000) *Histochem. Cell Biol.* **114,** 69–75
3. Barrett, K. E., and Keely, S. J. (2000) *Annu. Rev. Physiol.* **62,** 535–572
4. Taylor, C. J., McGaw, J., Howden, R., Duerden, B. I., and Baxter, P. S. (1990) *Arch. Dis. Child* **65,** 175–177
5. Baxter, P. S., Dickson, J. A., Variend, S., and Taylor, C. J. (1988) *Arch. Dis. Child* **63,** 1496–1497
6. Ameen, N., and Apodaca, G. (2007) *Traffic* **8,** 998–1006
7. Golin-Bisello, F., Bradbury, N., and Ameen, N. A. (2005) *Am. J. Physiol. Cell Physiol.* **289,** C708–C716
8. Bertrand, C. A., and Frizzell, R. A. (2003) *Am. J. Physiol. Cell Physiol.* **285,** C1–C18
9. Ameen, N., Silvis, M., and Bradbury, N. A. (2007) *J. Cyst Fibros.* **6,** 1–14
10. Silvis, M. R., Bertrand, C. A., Ameen, N., Golin-Bisello, F., Butterworth, M. B., Frizzell, R. A., and Bradbury, N. A. (2009) *Mol. Biol. Cell* **8,** 2337–2350
11. Naren, A. P., Di, A., Cormet-Boyaka, E., Boyaka, P. N., McGhee, J. R., Zhou, W., Akagawa, K., Fujiwara, T., Thome, U., Engelhardt, J. F., Nelson, D. J., and Kirk, K. L. (2000) *J. Clin. Invest.* **105,** 377–386
12. Guggino, W. B., and Stanton, B. A. (2006) *Nat. Rev. Mol. Cell Biol.* **7,** 426–436
13. Buss, F., Spudich, G., and Kendrick-Jones, J. (2004) *Annu. Rev. Cell Dev. Biol.* **20,** 649–676
14. Apodaca, G. (2001) *Traffic* **2,** 149–159
15. Ameen, N. A., van Donselaar, E., Posthuma, G., de Jonge, H., McLaughlin, G., Geuze, H. J., Marino, C., and Peters, P. J. (2000) *Histochem Cell Biol.* **114,** 219–228
16. Morris, S. M., Arden, S. D., Roberts, R. C., Kendrick-Jones, J., Cooper, J. A., Luzio, J. P., and Buss, F. (2002) *Traffic* **3,** 331–341
17. Mishra, S. K., Keyel, P. A., Hawryluk, M. J., Agostinelli, N. R., Watkins, S. C., and Traub, L. M. (2002) *EMBO J.* **21,** 4915–4926
18. Buss, F., and Kendrick-Jones, J. (2008) *Biochem. Biophys. Res. Commun.* **369,** 165–175
19. Morris, S. M., and Cooper, J. A. (2001) *Traffic* **2,** 111–123
20. Traub, L. M. (2003) *J. Cell Biol.* **163,** 203–208
21. Maldonado-Báez, L., and Wendland, B. (2006) *Trends Cell Biol.* **16,** 505–513
22. Morris, S. M., Tallquist, M. D., Rock, C. O., and Cooper, J. A. (2002) *EMBO J.* **21,** 1555–1564
23. Mishra, S. K., Hawryluk, M. J., Brett, T. J., Keyel, P. A., Dupin, A. L., Jha, A., Heuser, J. E., Fremont, D. H., and Traub, L. M. (2004) *J. Biol. Chem.* **279,** 46191–46203
24. Jha, A., Agostinelli, N. R., Mishra, S. K., Keyel, P. A., Hawryluk, M. J., and Traub, L. M. (2004) *J. Biol. Chem.* **279,** 2281–2290
25. Weixel, K., and Bradbury, N. A. (2002) *Methods Mol. Med.* **70,** 323–340
26. Peterson, M. D., and Mooseker, M. S. (1992) *J. Cell Sci.* **102,** 581–600
27. Peterson, M. D., Bement, W. M., and Mooseker, M. S. (1993) *J. Cell Sci.* **105,** 461–472
28. Nagai, J., Christensen, E. I., Morris, S. M., Willnow, T. E., Cooper, J. A., and Nielsen, R. (2005) *Am. J. Physiol. Renal Physiol.* **289,** F569–F576
29. Spudich, G., Chibalina, M. V., Au, J. S., Arden, S. D., Buss, F., and Kendrick-Jones, J. (2007) *Nat. Cell Biol.* **9,** 176–183
30. Bradbury, N. A., Cohn, J. A., Venglarik, C. J., and Bridges, R. J. (1994) *J. Biol. Chem.* **269,** 8296–8302
31. Weixel, K. M., and Bradbury, N. A. (2001) *Pflugers Arch.* **443,** (Suppl. 1) S70–S74
32. Swiatecka-Urban, A., Boyd, C., Coutermarsh, B., Karlson, K. H., Barnaby, R., Aschenbrenner, L., Langford, G. M., Hasson, T., and Stanton, B. A. (2004) *J. Biol. Chem.* **279,** 38025–38031
33. Prince, L. S., Peter, K., Hatton, S. R., Zaliauskiene, L., Cotlin, L. F., Clancy, J. P., Marchase, R. B., and Collawn, J. F. (1999) *J. Biol. Chem.* **274,** 3602–3609
34. Hu, W., Howard, M., and Lukacs, G. L. (2001) *Biochem. J.* **354,** 561–572
35. Weixel, K. M., and Bradbury, N. A. (2001) *J. Biol. Chem.* **276,** 46251–46259
36. Gotoh, N., Yan, Q., Du, Z., Biemesderfer, D., Kashgarian, M., Mooseker, M. S., and Wang, T. (2010) *Cytoskeleton* **67,** 178–192